

- [16] R. Riesenfeld. Applications of B-spline approximation to Geometric Problems of Computer-Aided Design. Ph.D. thesis. University of Utah Technical Report UTEC-CSc-73-126, March 1973.
  
- [17] D. F. Rogers and J. A. Adams. Mathematical Elements for Computer Graphics, second edition. McGraw-Hill Publishing Company, 1990.

- [7] E. Cohen, T. Lyche, and L. Schumaker. Algorithms for Degree Raising for Splines. *ACM Transactions on Graphics*, Vol 4, No 3, pp.171-181, July 1986.
- [8] E. Cohen, T. Lyche, and R. Riesenfeld. Discrete B-splines and subdivision Techniques in Computer-Aided Geometric Design and Computer Graphics. *Computer Graphics and Image Processing*, 14, 87-111 (1980).
- [9] M. D. Carmo. *Differential Geometry of Curves and Surfaces*. Prentice-Hall 1976.
- [10] I. D. Faux and M. J. Pratt. *Computational Geometry for Design and Manufacturing*.
- [11] G. Elber and E. Cohen. Error Bounded Variable Distance Offset Operator for Free Form Curves and Surfaces. *International Journal of Computational Geometry and Applications*, Vol. 1., No. 1, pp 67-78, March 1991.
- [12] G. Elber and E. Cohen. Second Order Surface Analysis Using Hybrid Symbolic and Numeric Operators Submitted for publication.
- [13] G. Elber. Free Form Surface Analysis using a Hybrid of Symbolic and Numeric Computation. Ph.D. thesis, University of Utah, Computer Science Department, 1992.
- [14] T. McCollough. Support for Trimmed Surfaces. M.S. thesis, University of Utah, Computer Science Department, 1988.
- [15] R. Millman and G. Parker. *Elements of Differential Geometry*. Prentice Hill Inc., 1977.

Assembly is left to the enjoyment of the author and other model building enthusiasts.

## 6 Acknowledgment

The author is grateful to Elaine Cohen and Mark Bloomenthal for their valuable remarks on the various drafts of this paper.

## References

- [1] RE Barnhill, G. Farin, L. Fayard and H. Hagen. Twists, Curvatures and Surface Interrogation. *Computer Aided Design*, vol. 20, no. 6, pp 341-346, July/August 1988.
- [2] B. O'Neill. *Elementary Differential Geometry*. Academic Press Inc., 1966.
- [3] C. Bennis, J. M. Vezien, and G. Iglesias. Piecewise Surface Flattening for Non-Distorted texture Mapping. *Computer Graphics*, Vol. 25, Num. 4, Siggraph Jul. 1991.
- [4] B. Cobb. *Design of Sculptured Surfaces Using The B-spline representation*. Ph.D. thesis, University of Utah, Computer Science Department, June 1984.
- [5] E. Cohen. Some Mathematical Tools for a Modeler's Workbench *IEEE Computer Graphics and Applications*, pp 63-66, October 1983.
- [6] E. Cohen, T. Lyche, and L. Schumaker. Degree Raising for Splines. *Journal of Approximation Theory*, Vol 46, Feb. 1986.

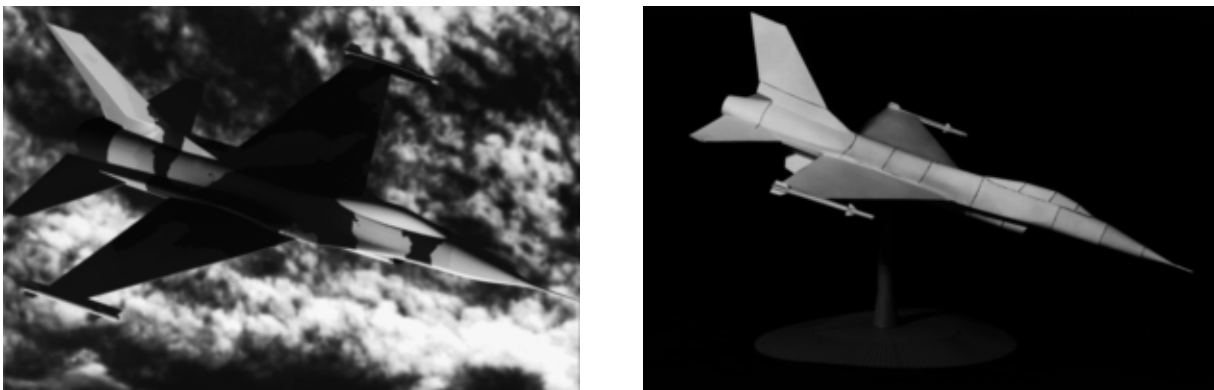


Figure 11: Computer model of an f16 (left) and assembled out of heavy paper (right).

Model	Time (Sec.)
Tube (figure 6)	1.4
Pawn (figure 9)	3
Teapot (figure 10)	5
Helicopter (figure 8)	7
f16 (figure 11)	150

Table 1: Different models layout construction times.

piecewise developable surfaces. However, the introduced approach allows one to construct a piecewise developable surface approximation to an arbitrary freeform surface, with tolerance control.

Throughout this paper, it was implicitly assumed that the material thickness is negligible. Unfortunately, this is not always the case and compensating for the distortion that can result is a future research topic. In addition, extending this methodology to support stretching and tearing, should be investigated. Not only will that enable dealing with arbitrary surfaces (which cannot be exactly decomposed into piecewise developable surfaces) but this algorithm may then support the ability to handle fabric and other anisotropic materials.

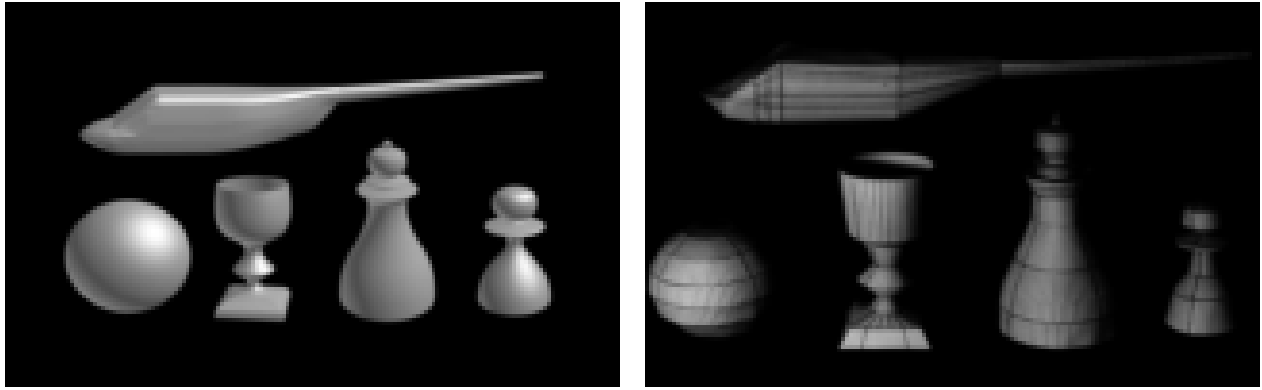


Figure 9: Computer models (left) and assembled out of heavy paper (right).



Figure 10: Computer model of a teapot (left) and assembled out of heavy paper (right).

and 11 show more complex models having several trimmed surfaces.

Table 1 provides some timing results for the model decomposition and layout computation. Tests were run on a SGI4D 240 GTX (R3000 25MHz Risc machine). All tests are measured in seconds.

## 5 Conclusion

This paper introduces a new approach to and provides a working algorithm for automating the decomposition and subsequent specification and layout of freeform models into developable components. Not every freeform surface can be exactly represented using

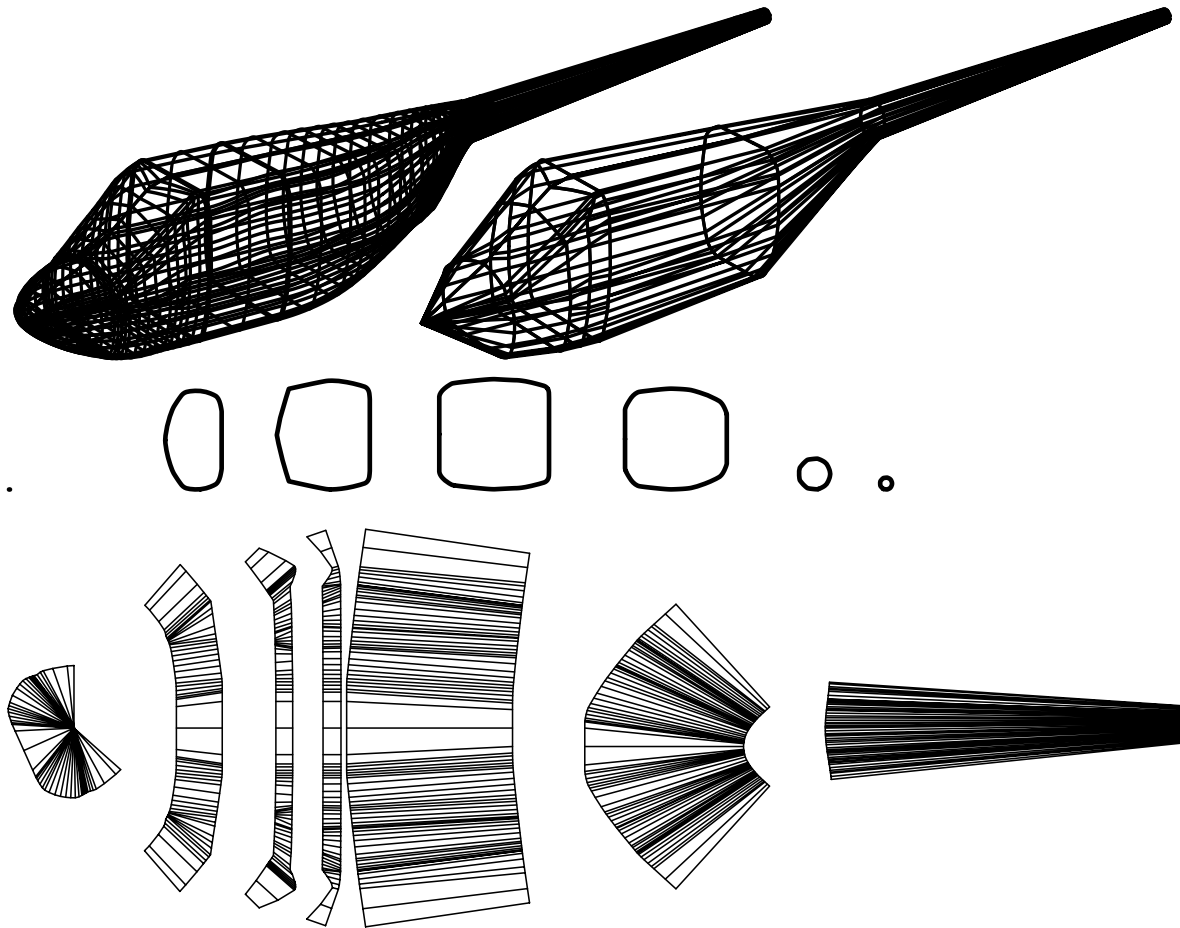


Figure 8: A helicopter model (top left) laid out (bottom) and assembled (top right).

projection with the cross sections of the developable surfaces, and the assembled piece.

Figure 9 shows several models laid out using these techniques and then assembled from heavy paper. Each developable surface was cut from paper and folded into its 3-space shape. Paper connecting stubs were used to hold and keep the pieces together.

More complex models can be created using Boolean operations when the model is a union or intersection of several freeform surfaces. The layouts of the trimming curves of these surfaces are also computed, in a way similar to the ruled surface layouts. Figures 10

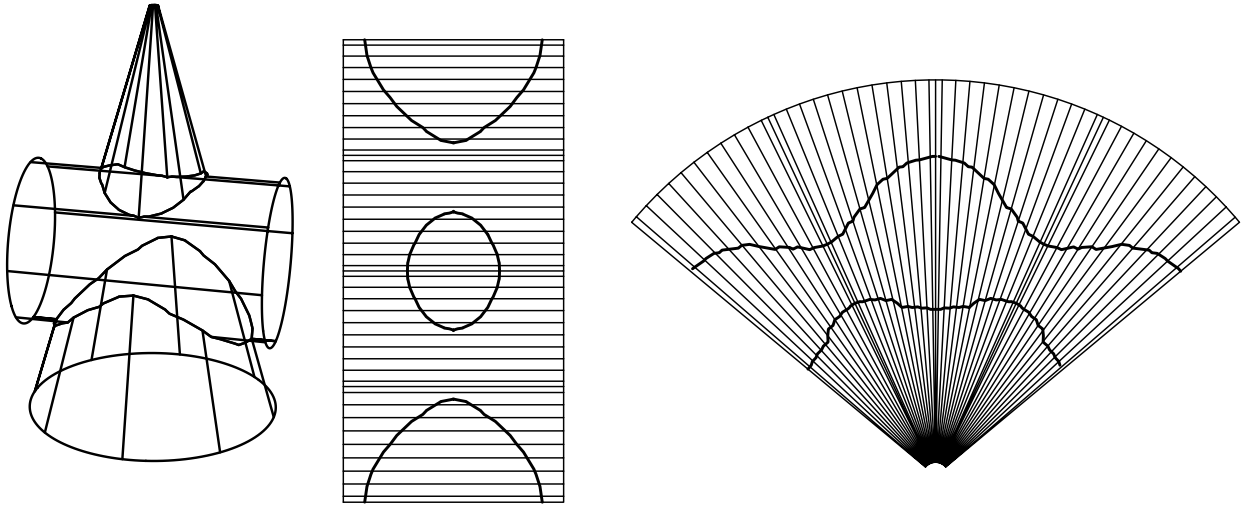


Figure 7: Trimming curves should be laid out with the ruled surfaces.

bilinear surface the  $u$  direction is also assumed to be of constant speed and the exact location is then interpolated from the flat bilinear four corner points. Finally, since the developable surface representation is only an approximation, it may be desired to re-execute the Boolean operations on the approximation. Appropriate trimming curves will be re-created for the fabrication surfaces of the approximation instead of the original surfaces. Figure 7 shows a simple layout with trimming curves and section 4 provides several examples of more complex models composed of trimmed surfaces as well.

## 4 Examples

The algorithm developed was used to generate layouts for several computer models, automatically. Figure 3 shows the sphere layout on a plane with its 3 dimensional piecewise ruled surface approximation. Figure 6 shows the layout of the model in figure 2 with an example of stubs. Figure 7 shows the layout of a cone and a cylinder intersecting each other with their trimming curves. Figure 8 shows a helicopter model [5], its layout

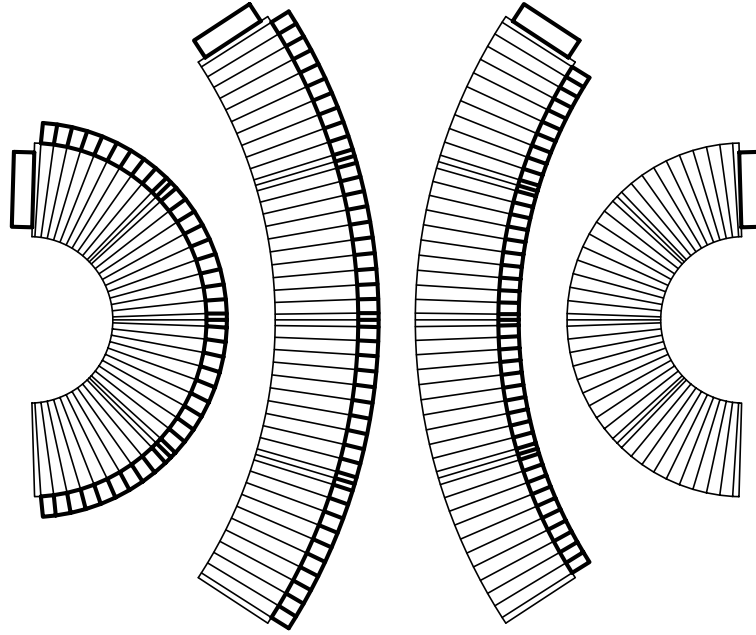


Figure 6: Stubs can be created by offsetting the planar boundary curves.

and 11.

When Boolean operators are applied to freeform models, trimmed surfaces result [14], and only part of each tensor product surface is used in the final model. In order to approximate freeform trimmed surfaces with piecewise developable surfaces, it is necessary to position the trimming curves in the plane with the developable surfaces. The problem is equivalent to finding the corresponding location of a specific surface Euclidean point in the planar representation of a developable surface, given the (trimming curve) point in the parametric space of the surface. With the added constraint that the surface speed in the  $v$  direction must be constant to within a prespecified tolerance, locating the given  $(u, v)$  point in the planar developable surface becomes a simplified problem. Since the  $u$  direction is approximated as piecewise linear in the laying out stage, a binary search in  $u$  can efficiently reveal the bilinear segment containing the point. Within the

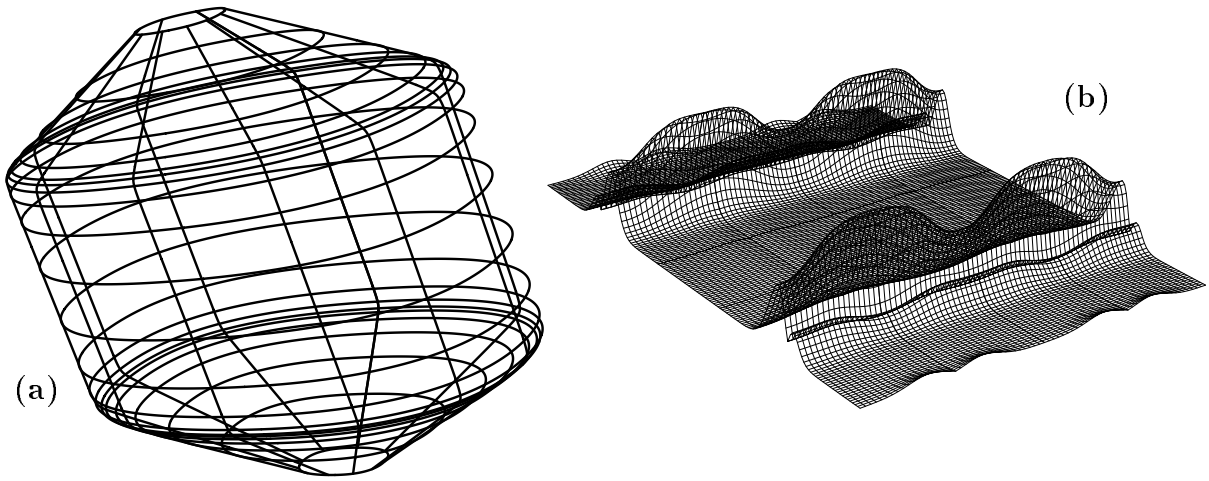


Figure 5:  $\kappa_n^v(u, v)$  (b) is used to determine where to subdivide the surface (a).

regions in the  $v$  direction (figure 5 (a)). Those regions are very noticeable in the  $\kappa_n^v(u, v)$  (figure 5 (b)) computed for this surface. Therefore,  $\kappa_n^v(u, v)$  can be used to automate a scheme that makes a more optimal ruled surface approximation.

In some cases, the laid out ruled surfaces can be insufficient to assemble the model, depending upon the assembly method. Some extra material might need to be included as stubs so the pieces may be stitched or welded together. Such stubs can be constructed by offsetting [11] the boundary curves of the planar representation of the approximating ruled surfaces. Figure 6 shows an examples of stubs generated using this approach that can be used for the layout of figure 2 (c). However, such stubs can cause a  $C^0$  seam between two folded developed surfaces resulting in a little stair with height equal to the material thickness. An alternative approach would be to connect two adjacent ruled surfaces using a separate stub made to span the two surfaces, from underneath, eliminating the stair. This last method was used in all the paper models in Figures 9, 10,

where  $s$  is the arc length parameterization of  $C$ . Since  $\langle u, (v \times w) \rangle = \langle (u \times v), w \rangle$

$$\begin{aligned}
 \kappa \langle N, n \rangle &= \frac{\left\langle \left( \frac{dC}{dt} \times \frac{d^2C}{dt^2} \right) \times \frac{dC}{dt}, n \right\rangle}{\left( \frac{ds}{dt} \right)^4} \\
 &= \frac{\left\langle \left( \frac{dC}{dt} \times \frac{d^2C}{dt^2} \right), \left( \frac{dC}{dt} \times n \right) \right\rangle}{\left( \frac{ds}{dt} \right)^4} \\
 &= \frac{\left\langle \left( \frac{dC}{dt} \times n \right), \left( \frac{dC}{dt} \times \frac{d^2C}{dt^2} \right) \right\rangle}{\left( \frac{ds}{dt} \right)^4} \\
 &= \frac{\left\langle \left( \frac{dC}{dt} \times n \right) \times \frac{dC}{dt}, \frac{d^2C}{dt^2} \right\rangle}{\left( \frac{ds}{dt} \right)^4} \\
 &= \frac{\left\langle n, \frac{d^2C}{dt^2} \right\rangle}{\left( \frac{ds}{dt} \right)^2}, \\
 &= \kappa_n^v
 \end{aligned} \tag{7}$$

since  $\left\| \frac{dC}{dt} \right\| = \frac{ds}{dt}$  and  $n$  is orthogonal to  $\frac{dC}{dt}$ .

$\kappa_n^v$  can be symbolically represented as a scalar surface (see [12, 13]). Its isolated local maxima are the suggested preferred locations for the piecewise ruled surface approximation subdivision. For obvious reasons, a maximum occurring on the boundary is of no interest, but  $C^1$  discontinuities in the  $v$  parametric direction are likely candidates for subdivision locations. Therefore, a surface should first be preprocessed and subdivided at all locations where it is not  $C^1$  continuous.  $\kappa_n^v(u, v)$  should then be computed for the resulting  $C^1$  continuous sub-surfaces. If the original surface is not  $C^2$ ,  $\kappa_n^v$  will not even be  $C^0$ . Special care should be taken in evaluating  $\kappa_n^v$  along those discontinuous edges, since limits from both sides along the  $C^0$  discontinuities would converge to different values.

An example is provided in figure 5, which shows a surface with two very highly curved

curvature in the  $v$  direction (the direction in which the approximating surfaces are ruled),  $\kappa_n^v(u, v)$  can be computed symbolically. The maximum values of  $\kappa_n^v(u, v)$  can then be used as subdivision locations. See figure 5 for one such example. The normal curvature,  $\kappa_n$ , of  $S$  in tangent direction  $\frac{\partial S}{\partial u} \frac{\partial u}{\partial t} + \frac{\partial S}{\partial v} \frac{\partial v}{\partial t}$  is

$$\kappa_n = \frac{II(a, b)}{I(a, b)} = \frac{II(\delta)}{I(\delta)} = \frac{\delta L \delta^T}{\delta G \delta^T}, \quad (5)$$

where  $\delta = (\frac{\partial u}{\partial t}, \frac{\partial v}{\partial t}) = (a, b)$  and  $G$  and  $L$  are the matrices of the first ( $I$ ) and second ( $II$ ) fundamental forms [9, 10], respectively.

From equation (5), when  $\delta = (0, d)$ , that is, the tangent vector direction is  $d \frac{\partial S}{\partial v}$ ,

$$\begin{aligned} \kappa_n^v &= \frac{(0, d)L(0, d)^T}{(0, d)G(0, d)^T} \\ &= \frac{d^2 \left\langle n, \frac{\partial^2 S}{\partial v^2} \right\rangle}{d^2 \left( \frac{\partial S}{\partial v} \right)^2} \\ &= \frac{\left\langle n, \frac{\partial^2 S}{\partial v^2} \right\rangle}{\left( \frac{\partial S}{\partial v} \right)^2}. \end{aligned} \quad (6)$$

Equation (6) is the normal curvature of the surface in the  $v$  direction. Equation (6) is also geometrically the curvature vector of the  $v$  iso-curve projected in the surface normal direction. Let  $T$ ,  $N$ , and  $B$  be the tangent, normal, and binormal of curve  $C(t)$ , respectively. For a non-arclength parameterized regular curve  $C(t)$  (see [15]),

$$\kappa N = \kappa B \times T = \frac{\left( \frac{dC}{dt} \times \frac{d^2C}{dt^2} \right) \times \frac{dC}{dt}}{\left( \frac{ds}{dt} \right)^4},$$

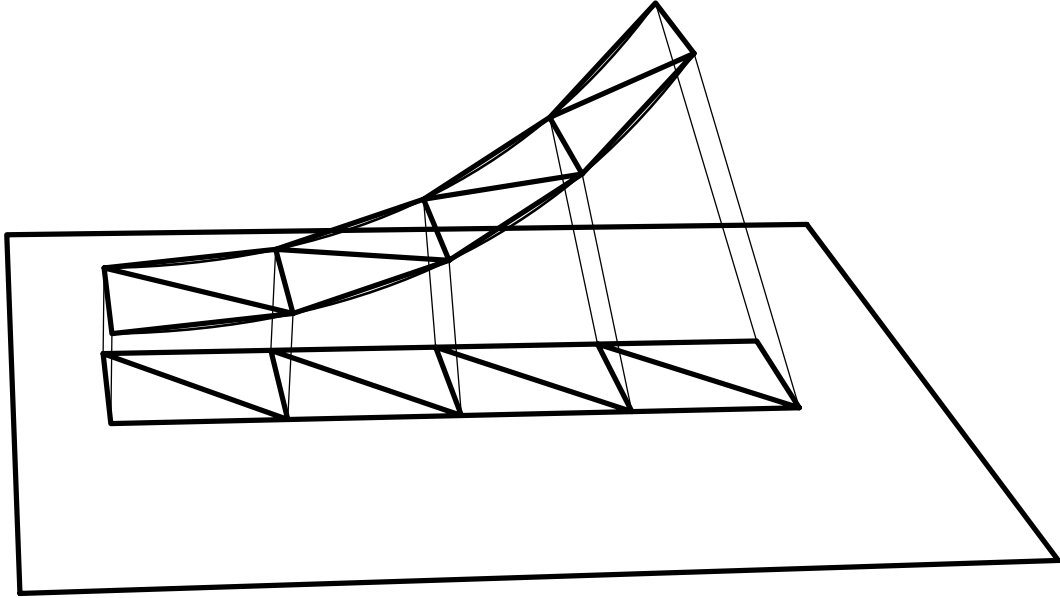


Figure 4: A ruled surface is approximated by triangles and unrolled onto a plane.

The process of laying down the surface can also be applied to a ruled surface that is not developable. By approximating the ruled surface using a set of triangles, as seen in Figure 4, we construct a developable polygonal approximation to the ruled surface. Further, the error in the approximation for the case of a ruled surface that is not developable can also be bounded using equation (4).

### 3 Extensions

It is a logical next step to improve the efficiency of algorithm 1 by subdividing  $S$  at  $v$  values that will minimize the number of ruled surfaces required to approximate  $S$  to within a given tolerance  $\tau$ . Automatically determining candidate locations is difficult. However, a greedy approach can be adopted to determine a local minimum even though it does not guarantee global minimum in the number of ruled surfaces. The normal

so they can be cut out. Lemma 1 can be used to verify whether the piecewise ruled surfaces are also developable. Since the isometry mapping is nonlinear, in general, an approximation must be used. We start the process by approximating the two boundary curves of  $R$  that originated on  $S$ ,  $C_1(u)$  and  $C_2(u)$ , as piecewise linear curves  $\hat{C}_1(u)$  and  $\hat{C}_2(u)$ , using refinement. An identical refinement should be computed and applied to both curves to insure they have the same number of linear segments,  $n$ . A one-to-one correspondence between the piecewise linear approximation of each curve is therefore established. Then, from each pair of corresponding linear segments, one from  $\hat{C}_1(u)$  and one from  $\hat{C}_2(u)$ , a bilinear surface is created. Each bilinear is further approximated as two triangles along one of the bilinear diagonals. Finally, the  $2n$  triangles are incrementally laid out and linearly transformed onto a plane (see figure 4).

Let the error of the triangular approximation be measured as the maximal distance between  $R$  and the triangular approximation, in a similar way to that of equation (3). Because  $R$  is a ruled surface, the maximal error must occur along one of the two boundaries of  $R$ ,  $C_1(u)$  and  $C_2(u)$  as,

$$\max \left\| \hat{C}_i(u) - C_i(u) \right\|, \quad i = 1, 2. \quad (4)$$

As stated above, the laying down of the surface is a non linear mapping and is only approximated. During the piecewise ruled surface approximation stage, it would be required to increase the number of ruled surfaces if a better approximation is necessary, complicating the assembly process. However, the penalty for a better layout approximation is reduced to only an enlargement of the data set.

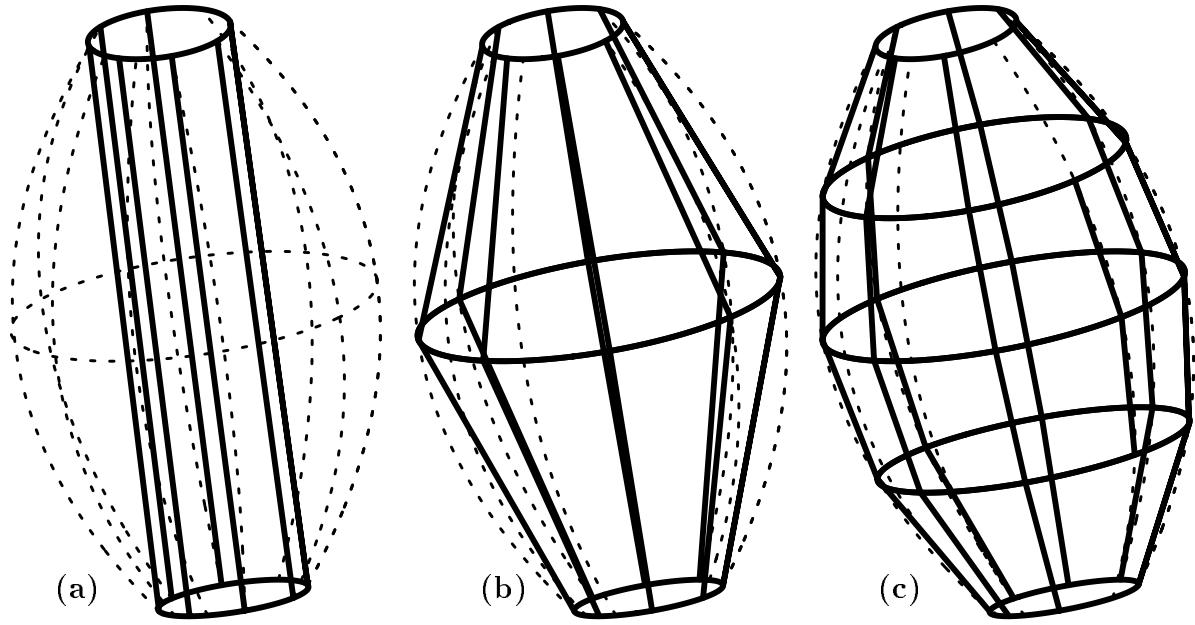


Figure 2: Three stages in approximating a surface with piecewise ruled surfaces (alg. 1).

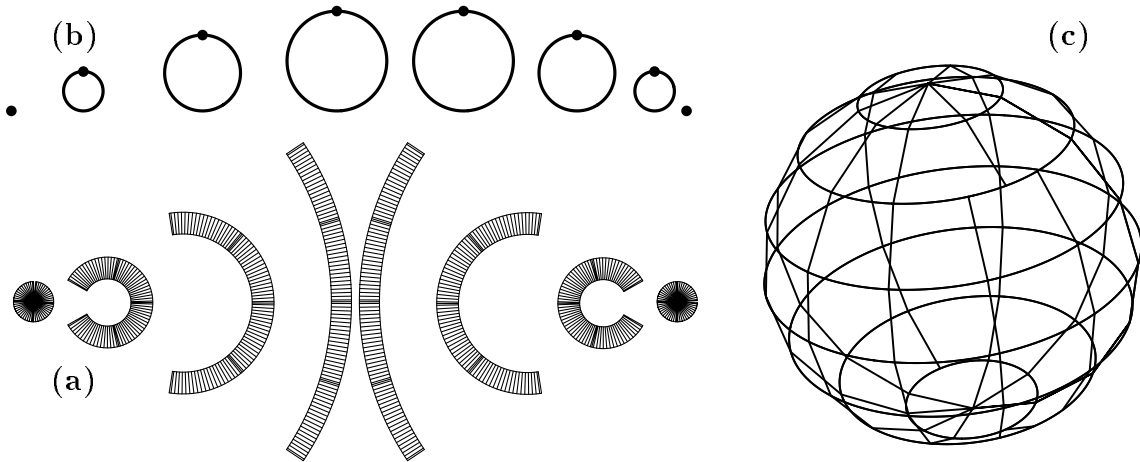


Figure 3: Piecewise developable surface approximation layout of a sphere (a), the cross sections of the developable approximation (b), and assembled (c).

of rings than as a sequence of elongated strips. A third consideration may be whether the surface is closed in one direction or not. Such closed surfaces are very common, and it is very natural to approximate such surfaces as a set of rings (see figures 2 and 3).

Once the set of ruled surfaces is determined, the surfaces must be laid flat on a plane,

**Algorithm 1**

Input:

$S(u, v)$ , surface to be divided in the  $v$  parametric direction.  
 $\tau$ , tolerance of approximation to be used.

Output:

$\mathcal{S}$ , Set of ruled surfaces, approximating  $S(u, v)$  to within  $\tau$ .

Algorithm:

```

RuledSrfApproximation(  $S$ ,  $\tau$  )
begin
   $C_1(t), C_2(t) \Leftarrow Vmin$  and  $Vmax$  boundary of  $S$ .
   $R \Leftarrow$  ruled surface between  $C_1(t)$  and  $C_2(t)$ .
   $\hat{R} \Leftarrow R$  refined and degree raised in  $v$ .
  If (  $\maxDistance( S, \hat{R} ) < \tau$  )
    return {  $R$  }.
  else
    begin
      Subdivide  $S$  into two subsrfs  $S^1, S^2$  along  $v$ .
    return
      RuledSrfApproximation(  $S^1$ ,  $\tau$  )  $\cup$ 
      RuledSrfApproximation(  $S^2$ ,  $\tau$  )
    end
end
end

```

parametric domain in each iteration, it halves the Euclidean bound in each iteration as well, so convergence in algorithm 1 is guaranteed. Note that we are concerned only with the  $v$  (ruled) direction since the representation is exact in the  $u$  direction.

Therefore, the less complex parametric direction, by some norm, may be a better candidate to select for the ruling direction approximation. Another measure for the selection of the subdivision direction may be the feasibility of the surface assembly. If  $S$  is an elongated tube, it may be easier to select and assemble the surfaces as sequence

mesh of  $S$ ,  $P_{\bullet j}$ , onto the line connecting  $P_{0j}$  and  $P_{mj}$  (b). The new ruled surface,  $\hat{R}$ , constructed with this new spacing is shown in Figure 1 (c).

The added degree of freedom of a non uniform  $v$  speed ruled surface approximation includes the uniform  $v$  speed ruled surface as a special case and so can always be as good approximation as the uniform speed approximation. Let  $C_1(v)$  and  $C_2(v)$  be two isoparametric curves of  $S$  in the  $v$  direction. Since we consider only one column of  $S$  mesh, this strategy will be able to emulate  $S$   $v$  speed well only if  $\left\| \frac{dC_1(v)}{dv} \right\| / \left\| \frac{dC_2(v)}{dv} \right\|$  is almost constant for all  $v$ . This condition holds fairly well for large classes of surfaces, but will not necessarily hold for surfaces constructed via highly non-isometric operations such as a warp [4]. However, it does eliminate the need for degree raising or refinement in the construction of  $\hat{R}$ , since the continuity (knot vector) of  $S$  in the  $v$  direction is inherited.

A distance bounded algorithm approximating an arbitrary tensor product surface as a set of ruled surfaces is derived in algorithm 1 based on this process.

Algorithm 1 returns a set of ruled surfaces that approximates the original surface  $S$  to within the required tolerance  $\tau$ . Figure 2 shows an example of three consecutive stages of algorithm 1.

Assuming  $S$  satisfies a Lipschitz condition, which automatically holds for B-spline surfaces, let  $(\frac{\Delta X}{\Delta v}, \frac{\Delta Y}{\Delta v}, \frac{\Delta Z}{\Delta v})$  be an upper bound on the first partial derivatives of  $S$  in the  $v$  direction. Given a finite range in the  $v$  parametric direction,  $\mathcal{V}$ , a bound on the Euclidean size is readily available as  $(\mathcal{V} \frac{\Delta X}{\Delta v}, \mathcal{V} \frac{\Delta Y}{\Delta v}, \mathcal{V} \frac{\Delta Z}{\Delta v})$ . Since algorithm 1 halves the

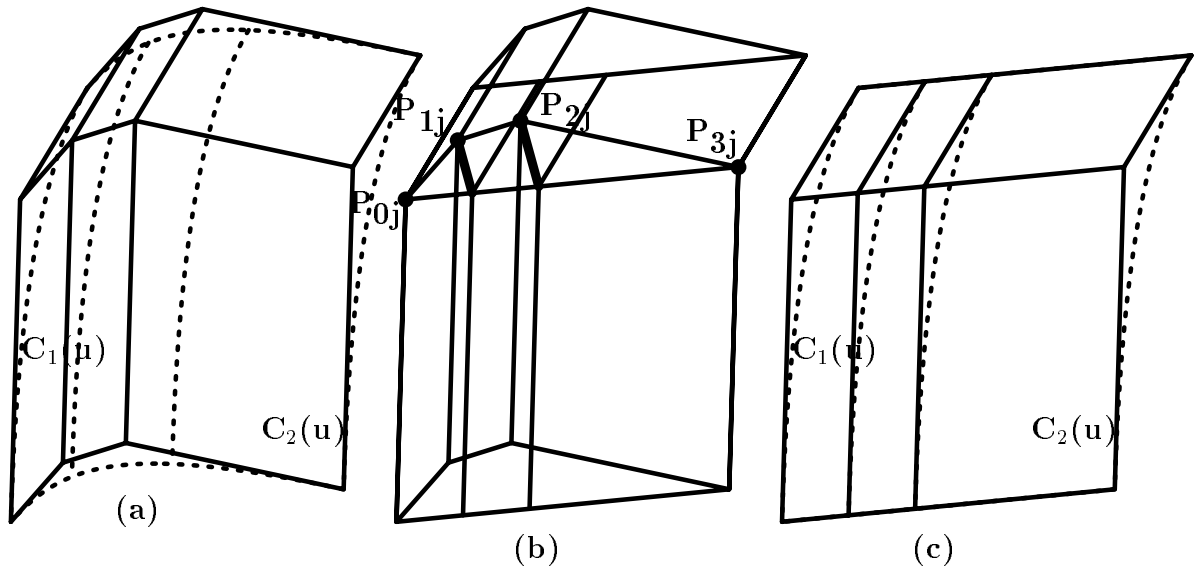


Figure 1: The speed of  $S$ 's isoparametric curve in the ruled direction is emulated by the ruled surface  $\hat{R}$  approximating it. In (a), the  $j$ th column of  $S$  mesh,  $P_{\bullet j}$ , is projected onto the line connecting  $P_{0j}$  and  $P_{mj}$  (b). The spacing of the projected points is used to construct the mesh of  $\hat{R}$ 's in (c).

method to correct for this problem uses the fact that control points can be associated with spline node values to obtain a surface-mesh parametric relation [16]. By degree raising  $R$  into  $\hat{R}$ , equally spaced in Euclidean space rows are introduced into the mesh that preserves the constant speed in the ruled direction,  $v$ . Since  $S$  does not have, in general, constant speed  $v$  isoparametric curves, one can consider unequal spacing of the introduced mesh rows. Such strategy can project a single column in the  $v$  direction of the control mesh of  $S$ ,  $P_{\bullet j}$ , onto the linear segment connecting  $P_{0j}$  and  $P_{mj}$  which are also control points of  $C_1(u)$  and  $C_2(u)$  respectively (see Figure 1). The spacing of these projected points can then be used to place the interior control points of  $\hat{R}$ . Figure 1 demonstrates this process. Figure 1 (a) has the original surface  $S$ . The control mesh of  $S$  is used in Figure 1 (b) to define the mesh of  $\hat{R}$ , by projecting a single column of the

of  $S(u, v)$ .  $\hat{R}(u, v)$  can be obtained from  $R(u, v)$  via appropriate degree raising [6, 7] and refinement [8] in the linear (ruled) direction,  $v$ . Then,

$$\begin{aligned}
\|S(u, v) - \hat{R}(u, v)\| &= \left\| \sum_{i=0}^m \sum_{j=0}^n P_{ij} B_{i,\tau}^m(u) B_{j,\xi}^n(v) - \sum_{i=0}^m \sum_{j=0}^n Q_{ij} B_{i,\tau}^m(u) B_{j,\xi}^n(v) \right\| \\
&= \left\| \sum_{i=0}^m \sum_{j=0}^n (P_{ij} - Q_{ij}) B_{i,\tau}^m(u) B_{j,\xi}^n(v) \right\| \\
&\leq \max(\|P_{ij} - Q_{ij}\|, \forall i, j),
\end{aligned} \tag{3}$$

since the B-spline basis functions are nonnegative and sum to one.

The difference of two rational surfaces can be computed in a similar way although it is more complex and must deal with products of scalar surfaces when the two are brought to a common denominator [13].

From the way  $\hat{R}$  is constructed it is clear that the first row of  $S$  control mesh is the same as the first row of  $\hat{R}$  control mesh, that is  $P_{0j} = Q_{0j} \forall j$ . Similarly, the last row of  $S$  control mesh is the same as the last row of  $\hat{R}$  control mesh, that is  $P_{mj} = Q_{mj} \forall j$ . The  $j$ th column of  $S$  control mesh will be referred to as  $P_{\bullet j}$ . Equation (3) provides a simple mechanism to bound the maximum distance between  $S$  and the ruled surface  $R$ .

Isoparametric curves of  $R$  (and  $\hat{R}$ ) in the ruled parametric direction have constant speed since  $R$  is linear in this parameter. The bound in equation (3) provides a good bound of the distance when the  $v$  isoparametric curves of  $S$  also have constant speed, that is when  $\|\frac{\partial S(u_0, v)}{\partial v}\| = c$ , for all  $u_0$ .

Unfortunately, when  $\frac{\partial S}{\partial v}$  is not constant, the number of ruled surfaces in the resulting approximation can be unnecessarily large in order to meet the required tolerance. A

“crosstalk” in the parameterization. Equation (2) measures this “crosstalk” projected in the direction of the surface normal.

Assuming one can approximate a given surface by a set of disjoint (except along boundaries) piecewise ruled surfaces within a prescribed tolerance, lemma 1 can be used to verify that each member of the set of ruled surfaces is also developable. Each developable surface can then be unfolded, laid flat and cut from a planar sheet such as paper or metal. In section 2, we also consider the case in which a ruled surface is not developable and present an approximation scheme with a tolerance control. By folding each laid down surface back to its Euclidean orientation and stitching them all together, a  $C^0$  approximation of the computer model is constructed.

Section 2 develops the background required for this method, and presents the basic algorithm. In section 3, we investigate several possible extensions including optimization, stub generation, and handling of trimmed surfaces. Section 4 lays out several examples including some models assembled from paper.

All the examples throughout this paper were created using an implementation that is based on the Alpha\_1 solid modeler, developed at the University of Utah.

## 2 Algorithm

Let  $S(u, v)$  be a nonuniform polynomial B-spline surface. Let  $C_1(u) = S(u, Vmin)$  and  $C_2(u) = S(u, Vmax)$  be the  $Vmin$  and  $Vmax$  boundary curves of  $S(u, v)$  respectively,  $C_1(u) \neq C_2(u)$ . Let  $R(u, v)$  be the ruled surface constructed between  $C_1(u)$  and  $C_2(u)$ . Let  $\hat{R}(u, v)$  be the representation for  $R(u, v)$  in the same B-spline basis as that

first concentrate on a superset of it, namely the class of ruled surfaces. In order to be able to use ruled surfaces instead, we need to derive the conditions in which a ruled surface is also developable. Let  $|G|$  and  $|L|$  be the determinants of the first and second fundamental form [2, 9], respectively.

**Lemma 1** *Let  $R$  be a regular ruled surface,  $R(u, v) = C_1(u) * v + C_2(u) * (1 - v)$ ,  $v \in (0, 1)$ .  $R$  is developable if and only if  $\left\langle n_r, \frac{\partial^2 R}{\partial u \partial v} \right\rangle \equiv 0$ ,*

**Proof:** Given a regular surface  $S$ , its Gaussian curvature,  $K$ , is zero everywhere (therefore, it is developable) if  $|L| \equiv 0$  since  $K = \frac{|L|}{|G|}$ , and  $|G| \neq 0$  for regular surfaces.

$$|L| = \left\langle n, \frac{\partial^2 S}{\partial u^2} \right\rangle \left\langle n, \frac{\partial^2 S}{\partial v^2} \right\rangle - \left\langle n, \frac{\partial^2 S}{\partial u \partial v} \right\rangle^2. \quad (1)$$

By differentiating  $R$  twice in  $v$ , it is clear that  $\frac{\partial^2 R}{\partial v^2} \equiv 0$ . We can immediately rewrite  $|L|$  as

$$|L_R| = - \left\langle n_r, \frac{\partial^2 R}{\partial u \partial v} \right\rangle^2, \quad (2)$$

and the result follows. ■

Therefore, to determine if a ruled surface is developable, one can symbolically compute  $\sigma(u, v) = \left\langle n_r, \frac{\partial^2 R}{\partial u \partial v} \right\rangle$  (That is, represent the scalar surface  $\sigma(u, v)$  as a polynomial Bézier or piecewise-rational NURBs scalar surface. See [12, 13] for more) and make sure it is zero everywhere within a prescribed tolerance. In other words, using the convex hull property of the Bézier and NURBs representations, all the coefficients of the scalar surface  $\sigma(u, v)$  must be zero within a prescribed tolerance.

The mixed partials, also called the twist of the surface [1, 13], are a measure of the

and to a less extent to fabric-based industries” [17]. Parts of aircrafts and ships are assembled from piecewise planar sheets unidirectionally bent into their model positions. Certain fabric and leather objects are made using patterns made from planar sheets.

Since developable surfaces can be unrolled onto a plane without distortion, they can be cut from planar sheets, bent back into their final position, and stitched together.

In [3], a flattening approximation is computed for freeform surfaces to eliminate the distortion in texture mapping. Surfaces are split into patches along feature (geodesic) lines and approximated as flats. However, we are mainly interested in isometric projections that preserves intrinsic distances and angles [2, 9]. Physically, such maps only bend the surface with no stretching, tearing, or distortion. One of the most interesting properties of developable surfaces is their ability to be laid flat on a plane without distortion by simply unrolling them [9, 10]. Therefore, we would like to generate a surface approximation using piecewise developable surfaces [9, 10], for which an isometric map to a plane exists.

Currently, the process that determines how and where to decompose the model requires human ingenuity and does not provide a bound on the accuracy of the approximation. This paper explores a technique for automatically decomposing the sculptured model, using a  $C^0$  approximation with error bound control, into sets of developable surfaces.

The Gaussian curvature of a developable surface  $S(u, v)$ ,  $K$ , is zero everywhere [9, 10], i.e.  $K(u, v) \equiv 0$ . The class of developable surfaces is difficult to deal with, so we will

# Model Fabrication using Surface Layout Projection \*

Gershon Elber<sup>†‡</sup>  
Department of Computer Science  
University of Utah  
Salt Lake City, UT 84112 USA

July 8, 1995

## Abstract

This paper presents a model fabrication scheme that automatically approximates a model whose boundary consists of several freeform surfaces by developable surfaces and then unroll these developable surfaces onto a plane. The model can then be fabricated by assembling the sets of developable surfaces which have been cut from planar sheets and rolled back to their proper Euclidean locations. Both the approximation and the rolling methods can be made arbitrarily precise.

## 1 Introduction

It is common to find freeform surfaces manually approximated and assembled as sets of piecewise developable surfaces [9]. In general, freeform surfaces are not developable and cannot be exactly represented as piecewise developable surfaces. Yet, “developable surfaces are of considerable importance to sheet-metal- or plate-metal-based industries

---

\*This work was supported in part by DARPA (N00014-91-J-4123). All opinions, findings, conclusions or recommendations expressed in this document are those of the authors and do not necessarily reflect the views of the sponsoring agencies.

<sup>†</sup>Appreciation is expressed to IBM for partial fellowship support of the author.

<sup>‡</sup>Current address: Computer Science Department, Technion, Haifa 32000, Israel